

Antiphase boundaries in $\text{Ba}_{0.75}\text{Sr}_{0.25}\text{TiO}_3$ epitaxial film grown on (001) LaAlO_3 substrate

Y. Q. Wang,^{1,a)} W. S. Liang,¹ Peter Kr. Petrov,² and Neil McN. Alford²

¹The Cultivation Base for State Key Laboratory, Qingdao University, No. 308 Ningxia Road, Qingdao 266071, People's Republic of China

²Department of Materials, Imperial College London, Exhibition Road, London SW7 2AZ, United Kingdom

(Received 28 December 2010; accepted 17 February 2011; published online 2 March 2011)

$\text{Ba}_{0.75}\text{Sr}_{0.25}\text{TiO}_3$ film was epitaxially grown on a (001) LaAlO_3 substrate using single-target pulsed laser deposition. The microstructure of the epitaxial film was investigated by conventional and high-resolution transmission electron microscopy. Apart from dislocations and stacking faults, two different kinds of antiphase boundaries, one being straight, and the other being zig-zagged, have been observed. The formation mechanism of these antiphase boundaries is discussed.

© 2011 American Institute of Physics. [doi:10.1063/1.3562972]

Ferroelectric thin films including BaTiO_3 , SrTiO_3 , and $(\text{Ba,Sr})\text{TiO}_3$ (BSTO) have received great attention because of their potential applications for various functional devices.^{1,2} Extensive research work has indicated that the dielectric properties of epitaxial BSTO thin film strongly depend on internal stress and defect structure.³⁻⁶ For BSTO thin films grown on a single-crystalline substrate such as LaAlO_3 , there is a lattice mismatch (about 3.8%) and difference in their thermal coefficients. These differences lead to the formation of dislocations, stacking faults (SFs), and antiphase domains in the epitaxial film. These defects could increase the dielectric loss and reduce the tuneability of the film. Thus, it is necessary to carry out a comprehensive investigation of the defect structures in epitaxial BSTO films.

In epitaxial perovskite thin films, edge type threading or misfit dislocations with a Burgers vector of $\mathbf{b}=\langle 100 \rangle$ or $\langle 110 \rangle$ have been observed.⁷⁻⁹ In addition, it has been found that the misfit or threading dislocations can dissociate into partial dislocations connected by a strip of SFs.⁹⁻¹¹ However, for BSTO/ LaAlO_3 system, only few experimental studies are available concerning the mechanism of misfit accommodation and generation of microstructural defects.

In this paper, we report a detailed microstructure investigation of $\text{Ba}_{0.75}\text{Sr}_{0.25}\text{TiO}_3$ film epitaxially grown on a (001) LaAlO_3 substrate by a single-target pulsed laser deposition (PLD) technique. Transmission electron microscopy (TEM) has been used in conventional mode and high-resolution mode (HRTEM) to investigate the microstructural defects in the epitaxial film. Apart from dislocations and SFs, two different kinds of antiphase boundaries (APBs) have been observed. The possible formation mechanism for two different kinds of APBs is discussed.

A 1- μm -thick film of $\text{Ba}_{0.75}\text{Sr}_{0.25}\text{TiO}_3$ was epitaxially grown on a (001) LaAlO_3 substrate using a single-target PLD technique. Targets for the PLD system were made from ceramic powder prepared using a mixed oxide route.¹² The substrate temperature was kept at 650 °C during the deposition. The film thickness was controlled by the number of pulses shot on the targets. Once the ablation was over, the samples were annealed for 1 h in an oxygen rich environment (760 Torr) in order to reduce the oxygen vacancies, and

then slowly cooled down to room temperature at a rate of 10 °C/min. The specimens for TEM examination were prepared in a cross-sectional orientation ([010] zone-axis for the LaAlO_3 substrate) using conventional techniques of mechanical polishing and ion thinning. The ion thinning was performed using a Gatan Model 691 Precision Ion Polishing System. The bright-field (BF) imaging, selected-area electron diffraction (SAED) and HRTEM examinations were carried out using a JEOL JEM 2100F transmission electron microscope operating at 200 kV.

Figure 1(a) is a typical BF TEM image of a cross-sectional $\text{Ba}_{0.75}\text{Sr}_{0.25}\text{TiO}_3/\text{LaAlO}_3$ sample. The inset in Fig. 1(a) is a typical SAED pattern taken from the epitaxial film

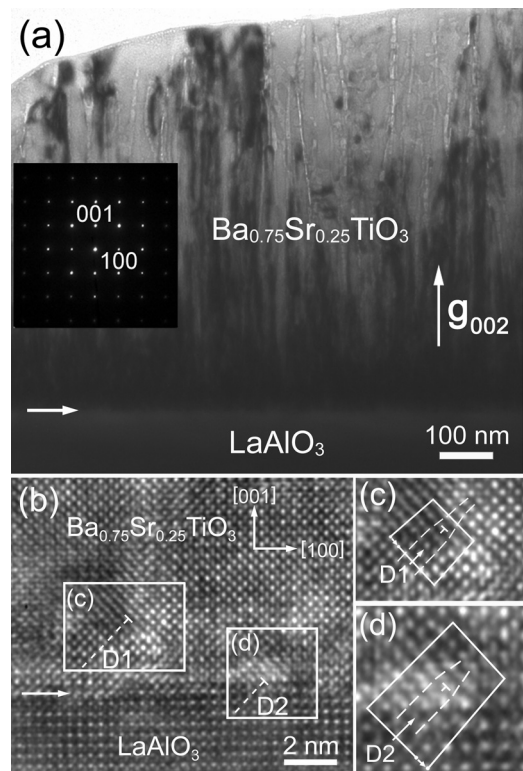


FIG. 1. (a) Cross-sectional BF TEM image of $\text{Ba}_{0.75}\text{Sr}_{0.25}\text{TiO}_3/\text{LaAlO}_3$. Inset shows [010] zone-axis SAED pattern taken from the film; (b) a typical HRTEM image of the interface region between $\text{Ba}_{0.75}\text{Sr}_{0.25}\text{TiO}_3$ and LaAlO_3 , showing two misfit dislocations indicated by D1 and D2; (c) Burgers circuit for D1; (d) Burgers circuit for D2.

^{a)}Author to whom correspondence should be addressed. Electronic mail: yqwang@qdu.edu.cn.

region, which corresponds to a $[010]$ zone-axis diffraction pattern of $\text{Ba}_{0.75}\text{Sr}_{0.25}\text{TiO}_3$ film. The BF image was taken under a two-beam condition with $\mathbf{g}=002$. It can be seen from Fig. 1(a) that there are many dislocations in the epitaxial film. Extensive tilting experiments indicated that most of the misfit or threading dislocations starting from the interface region are pure-edge types with Burgers vectors of $\langle 100 \rangle$ or $\langle 101 \rangle$, and they tend to dissociate into two partials with Burgers vectors of type $1/2\langle 101 \rangle$, bound by a strip of SFs. One example is shown in Fig. 1(b), which was taken near the $\text{Ba}_{0.75}\text{Sr}_{0.25}\text{TiO}_3/\text{LaAlO}_3$ interface region. It can be seen that misfit dislocations are not exactly located at the $\text{Ba}_{0.75}\text{Sr}_{0.25}\text{TiO}_3/\text{LaAlO}_3$ interface but inside the $\text{Ba}_{0.75}\text{Sr}_{0.25}\text{TiO}_3$ film a few monolayers away from the interface. Careful examination of Fig. 1(b) demonstrates that there are two extra half planes along the $[10\bar{1}]$ direction, indicating that they belong to pure-edge type dislocations. The extra half planes are indicated by dashed lines for D1 and D2 in Fig. 1(b). To determine the Burgers vectors for D1 and D2, Burgers circuits are drawn to enclose the dislocations in the enlarged HRTEM images of rectangle regions in Fig. 1(b). It can be clearly seen from Figs. 1(c) and 1(d) that there is a gap between the starting and ending point in each Burgers circuit, which is indicated by an arrow, respectively. The Burgers vectors for dislocations D1 and D2 are both determined to be $1/2[10\bar{1}]$.

Careful examination of Fig. 1(a) demonstrates that there are a lot of lighter lines in the top layer region. It can also be seen that some lighter lines even run up through the whole thickness of the epitaxial film. In addition, the contrast of the lines is completely different from that of misfit or threading dislocations. In order to clarify the nature of these lighter lines, extensive HRTEM examinations were carried out. HRTEM examinations showed that most of the lighter lines are originated from APBs, which is consistent with the previous report.¹³ In addition, two kinds of morphologies, one being straight, and the other being zig-zagged, have been observed for these APBs. More zig-zagged APBs are found in the $\text{Ba}_{0.75}\text{Sr}_{0.25}\text{TiO}_3$ epitaxial film.

Figure 2(a) shows an example of straight APBs in the epitaxial $\text{Ba}_{0.75}\text{Sr}_{0.25}\text{TiO}_3$ film. The three domains are indicated by A, B, and C, and the width of domain B is about 10 nm. The three white lines, which connect the brighter dots of (Ba, Sr) atoms, are on the same level for domains A and C, while the three lines of domain B show an evident shift in $(1/2)c$ along the $[001]$ direction. Two APBs are found, which are indicated by two arrows labeled with APB I and APB II in Fig. 2(a), respectively. The origin of the APBs can be attributed to the terrace or step on the surfaces of LaAlO_3 substrate. The schematic atomic structure for the straight APBs is shown in Fig. 2(b). Figure 2(c) shows the simulated HRTEM image for the straight APB, which matches the experimental image very well. The surface structure of (001) LaAlO_3 substrate can be regarded to consist of steps and terraces. The growth of epitaxial film can be considered to follow a two-dimensional layer-by-layer mode, and that is to say, the (Ba, Sr)O and TiO_2 layers are grown alternatively. When the terrace or step is equal to $(1/2)c$ of LaAlO_3 substrate, $\text{Ba}_{0.75}\text{Sr}_{0.25}\text{TiO}_3$ domains, like domain B, grown on the terrace will be displaced by $(1/2)c$ along the growth direction, compared with those neighboring grains grown on the normal surfaces, such as domains A and C. Consequently,

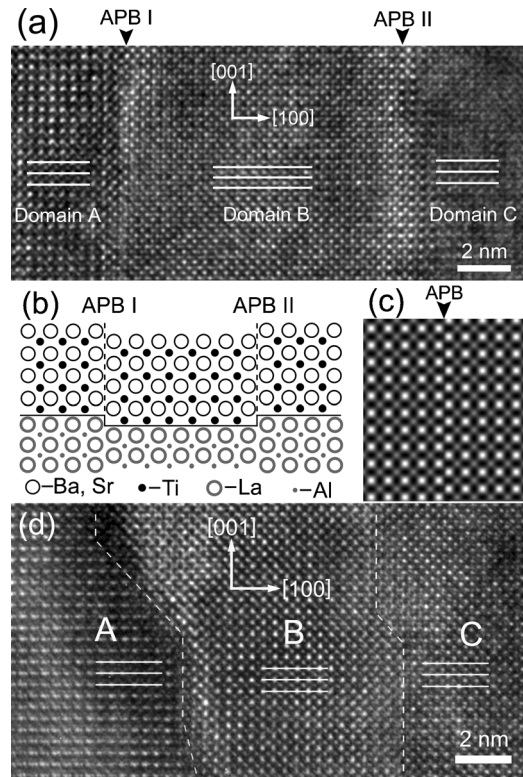


FIG. 2. (a) An example of straight APB; (b) schematic atomic structure for the straight APB; (c) simulated HRTEM image for the straight APB; (d) an example of zig-zagged APB.

a straight APB, which is parallel to the growth direction, will be formed. The formation of APB due to the presence of atomic steps has been found in Fe_3O_4 epitaxial films.^{14–16} In addition, similar defects have also been observed in the structurally-related Ruddlesden–Popper phases¹⁷ and non-stoichiometric SrTiO_3 thin film.¹⁸ Figure 2(d) shows an example of zig-zagged APBs in the epitaxial film. There are three domains, and the width of domain B is around 8 nm. It can be seen clearly that the three white lines, which connect the brighter dots of (Ba, Sr) atoms in domains A, C, and B, are not on the same level. In addition, the APB is not straight but zig-zagged, which is illustrated by the dashed lines in Fig. 2(d). Most of the zig-zagged boundaries are tilted around 45° from the $[001]$ direction. As mentioned above, the APB is caused by the terraces or steps on the surface of LaAlO_3 substrate. It should be noted that the islands grow in both vertical and lateral dimensions and coalesce to form a continuous $\text{Ba}_{0.75}\text{Sr}_{0.25}\text{TiO}_3$ film consequently. The initial island shape and the lateral growth rate determine whether the domain is straight or zig-zagged. When the lateral growth rate is not the same for two neighboring islands, irregular boundaries will form after the coalescence of two islands. A change in the boundaries orientation only requires low energy. That is why more zig-zagged APBs were observed. The shift vector of the APB is $1/2[001]$, which is around 1.9 \AA .

Figure 3(a) shows an example of more complex APBs in the epitaxial film. The boundary between domains A and B is indicated by two white arrows in Fig. 3(a). It can be seen that the atomic layers of (Ba, Sr)O in the two domains show a displacement of $(1/2)c$ along the $[001]$ direction. In order to demonstrate the displacement more clearly, an enlarged HRTEM image of the rectangle region in Fig. 3(a) is shown in Fig. 3(b). The APB is illustrated by the dashed lines, and the

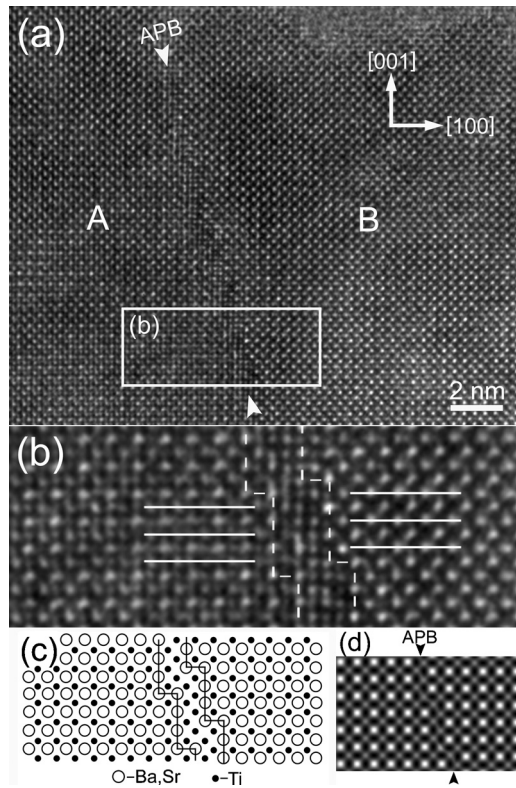


FIG. 3. (a) An example of more complex zig-zagged APB; (b) enlarged HRTEM image showing the lattice displacement; (c) schematic atomic structure for the complex APB; (d) simulated HRTEM image for the zig-zagged APB.

three white lines in the two domains clearly demonstrate a displacement of $1/2[001]$. The schematic atomic structure for the zig-zagged APB is shown in Fig. 3(c). Figure 3(d) shows the simulated HRTEM image for the zig-zagged APB, which is in good agreement with the experimental images. Careful examination of Figs. 3(a) and 3(b) shows that (101) fringes in domain A are shifted $1/4[101]$, and the $(10\bar{1})$ fringes in domain B are shifted $1/4[\bar{1}01]$. Thus the total displacement is $1/4[101] + 1/4[\bar{1}01] = 1/2[001]$. The formation mechanism of the complex zig-zagged APB is different from those shown in Fig. 2. There are many nucleation sites of $\text{Ba}_{0.75}\text{Sr}_{0.25}\text{TiO}_3$ located at different positions on the LaAlO_3 surface. If the nucleation site is just on the terrace, and two neighboring grains grow vertically simultaneously, a straight APB in Fig. 2 will form consequently. However, if the nucleation site is not just on the terrace but a little far away from the terrace, when the two islands grow laterally and consequently coalesce together, a complex zig-zagged APB in Fig. 3 will be produced. This is energetically favorable because nuclei prefer to form on the terraces or steps on the substrate surfaces.

APBs are usually formed during the disorder-order phase transformation. The LaAlO_3 substrate was kept at 923 K during the deposition process, and then cooled down to room temperature. If LaAlO_3 substrate is disordered at 923 K, then

APB could form in the substrate during the cooling process. But if it is still ordered at 923 K, then APB could not be produced in the substrate during the cooling process. For the straight APB, it has been reported in the BaTiO_3 epitaxial film grown on $\text{SrRuO}_3/\text{SrTiO}_3$.¹³ It was thought that these APBs act as a complementary mechanism to release local strains. However, for the zig-zagged APB, it has never been observed in $\text{BSTO}/\text{LaAlO}_3$ system before. The formation of the straight or zig-zagged APBs depends on the position of the nucleation sites on the substrate surface.

In conclusion, two kinds of APBs, one being straight and the other being zig-zagged in morphology, have been observed in $\text{Ba}_{0.75}\text{Sr}_{0.25}\text{TiO}_3$ film. The formation of the APBs is caused by two different mechanisms. If the nucleation site is just on the terrace, and two neighboring grains grow vertically simultaneously, a straight APB will be formed. However, if the nucleation site is not just on the terrace but a little far away from the terrace, when the two islands grow laterally and coalesce, a zig-zagged APB will be produced.

The authors would like to thank the financial support from the National Natural Science Foundation of China (Grant No. 10974105) and the Scientific Research Starting Foundation for the Introduced Talents at Qingdao University (Grant No. 06300701). Y. Q. Wang would also like to thank the financial support from Taishan Outstanding Overseas Scholar Program of Shandong Province. The authors are grateful to Professor Xiaofeng Duan at Institute of Physics, Chinese Academy of Sciences for his helpful discussion.

¹D. E. Kotecki, *Integr. Ferroelectr.* **16**, 1 (1997).

²K. Bouzouane, P. Woodall, B. Marchilhas, A. N. Khodan, D. Crete, E. Jacquet, J. C. Mage, and J. P. Contour, *Appl. Phys. Lett.* **80**, 109 (2002).

³S. Hyun, J. H. Lee, S. S. Kim, K. Char, S. J. Park, J. Sok, and E. H. Lee, *Appl. Phys. Lett.* **77**, 3084 (2000).

⁴T. R. Taylor, P. J. Hansen, B. Acikel, N. Pervez, R. A. York, S. K. Streiffner, and J. S. Speck, *Appl. Phys. Lett.* **80**, 1978 (2002).

⁵Z. G. Ban and S. P. Alpay, *J. Appl. Phys.* **93**, 504 (2003).

⁶N. A. Pertsev, A. G. Zembilgotov, and A. K. Tagantsev, *Phys. Rev. Lett.* **80**, 1988 (1998).

⁷X. Y. Qi, J. Miao, X. F. Duan, and B. R. Zhao, *Mater. Lett.* **60**, 2009 (2006).

⁸X. Y. Qi, J. Miao, X. F. Duan, and B. R. Zhao, *J. Cryst. Growth* **277**, 218 (2005).

⁹T. Suzuki, Y. Nishi, and M. Fujimoto, *Philos. Mag. A* **79**, 2461 (1999).

¹⁰C. J. Lu, L. A. Bendersky, K. Chang, and I. Takeuchi, *Philos. Mag.* **83**, 1565 (2003).

¹¹C. J. Lu, C. Li, Y. C. Zhang, W. N. Ye, F. K. Shan, and L. H. Xia, *J. Appl. Phys.* **106**, 113532 (2009).

¹²K. Sarma, R. Farooq, K. Jarman, R. Pullar, P. K. Petrov, and N. M. Alford, *Integr. Ferroelectr.* **62**, 249 (2004).

¹³J. Q. He, E. Vasco, R. Dittmann, and R. H. Wang, *Phys. Rev. B* **73**, 125413 (2006).

¹⁴S. Celotto, W. Eerenstein, and T. Hibma, *Eur. Phys. J. B* **36**, 271 (2003).

¹⁵S. K. Arora, R. G. S. Sofin, and I. V. Shvets, *Phys. Rev. B* **72**, 134404 (2005).

¹⁶V. V. Roddatis, D. S. Su, C. Kuhrs, W. Ranke, and R. Schlögl, *Thin Solid Films* **396**, 78 (2001).

¹⁷M. A. Zurbuchen, W. Tian, X. Q. Pan, D. Fong, S. K. Streiffner, M. E. Hawley, J. Lettieri, Y. Jia, G. Asayama, S. J. Fulk, D. J. Comstock, S. Knapp, A. H. Carim, and D. G. Schlom, *J. Mater. Res.* **22**, 1439 (2007).

¹⁸T. Suzuki, Y. Nishi, and M. Fujimoto, *Philos. Mag. A* **80**, 621 (2000).